Translational Oncology 28 (2023) 101614

Contents lists available at ScienceDirect

Translational Oncology

journal homepage: www.elsevier.com/locate/tranon

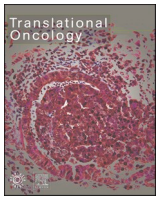

Original Research

Expression of glucose transporter-1 in follicular lymphoma affected tumor-infiltrating immunocytes and was related to progression of disease within 24 months

Yuwei Deng [a,1], Jianli Ma [b,1], Shu Zhao [a], Ming Yang [a], Yutian Sun [a], Qingyuan Zhang [c,*]

[a] Department of Medical Oncology, Harbin Medical University Cancer Hospital, Harbin, Heilongjiang 150081, People's Republic of China
[b] Department of Radiation Oncology, Harbin Medical University Cancer Hospital, Harbin, Heilongjiang 150081, People's Republic of China
[c] Department of Medical Oncology, Harbin Medical University Cancer Hospital, Heilongjiang Cancer Institute, Harbin, Heilongjiang 150081, People's Republic of China

ARTICLE INFO

Keywords:
GLUT1
Follicular lymphoma
POD24
Tumor-infiltrating immunocytes
PI3K/Akt /mTOR signaling

ABSTRACT

Objective: Follicular lymphoma (FL) occurring progression within 24 months (POD24) after initial immunochemotherapy has poor prognosis. GLUT1 affects glycolysis within tumor microenvironment (TME) and promotes tumor progression. However, its specific mediated mechanism remains unclear in FL.
Methods: Baseline GLUT1 expression, infiltrations of M2 macrophage, and CD8+ T-cells were assessed by immunohistochemistry in FL with POD24 and long-term remission respectively. The spatial features of TME were assessed by MIBI-TOF and proteomics. Predictive immunophenotypes for POD24 occurrence was analyzed by random forest algorithm. The lactate production and the induction of M2 macrophages were detected when GLUT1 was transfected or knocked down in DOHH2. The activation of PI3K/Akt/mTOR signaling in DOHH2 and WSU-FSCCL cells co-cultured with induced inhibitory immunocytes was tracked by western blotting.
Results: The FL with POD24 exhibited higher baseline GLUT1 expression and increased infiltration of various inhibitory immunocytes. Spatial signatures of 69 immunophenotypes could predict POD24 occurrence. The activation of PI3K/ Akt /mTOR signaling pathway was not significant in both groups. The supernatant of DOHH2-GLUT1 cells which had more lactate content could induce more M2-type macrophages than that of DOHH2/siRNA GLUT1 cells. When co-cultured with exhausted CD8+ T cells, M2-type macrophages and Tregs, compared with WSU-FSCCL cells, DOHH2 cells with high GLUT1 expression induced more M2-type macrophages and was triggered activation of PI3K/ Akt /mTOR signaling pathway.
Conclusion: Tumor cells overexpressing GLUT1 could domesticate immunocytes to form an immunosuppressive TME, which promotes occurrence of POD24 and gradually activates PI3K/ Akt /mTOR pathway of tumor cells in FL.
Significance: Tumor cells overexpressing GLUT1 could domesticate immunocytes to form an immunosuppressive microenvironment, which in turn promoted the growth of tumor cells and was related to the progression of disease within 24 months in FL. Suppressive immunocytes gradually activated PI3K/ Akt /mTOR pathway of tumor cells in later stage. Distinguishing spatial features of immunocytes could well predict POD24 occurrence, hoping to benefit these patients from early anti-metabolism therapy based on GLUT1 in the future.

Introduction

Follicular lymphoma (FL) is the most common indolent lymphoma displaying germinal center (GC) B cell differentiation, accounting for 10–20% of all non-Hodgkin lymphoma [1] and there are more than 15,000 new diagnosed patients each year in our country [2]. Follicular lymphoma is highly heterogeneous and although the majority of patients have a good prognosis, approximately 20% of patients occurred

Abbreviations: GLUT1, glucose transport protein 1; TME, tumor microenvironment; FL, follicular lymphoma; MIBI-TOF, multiplexed ion beam imaging by time of flight; POD24, progression of disease within 24 months.

* Corresponding author.
E-mail address: 0566@hrbmu.edu.cn (Q. Zhang).

[1] These authors contributed equally to this work.

https://doi.org/10.1016/j.tranon.2022.101614
Received 12 November 2022; Received in revised form 11 December 2022; Accepted 23 December 2022

progression of disease within 24 months (POD24) [3]. These patients progress rapidly with dismal prognosis. Due to lacking suitably early screening methods, they fail to receive targeted treatment. Therapeutic resistance in this setting acts as the essential feature of FL with POD24 [4]. It is a focus of lymphoma research to find effective therapeutic targets that can identify FL with POD24, and it is also the key to improve the overall treatment level of FL, which has important clinical significance.

FL International Lymphoma Prognostic Index (FLIPI) acts as a classifier to discover FL with POD24 which has a specificity of approximately 60%. However, about 40% with a high risk FLIPI at the initial diagnosis are found without subsequent POD24 [5]. Other methods, such as m7-FLIPI, circulating tumor cells, and circulating DNA, have been applied for prognosis of the disease, but not underlie therapeutic targets. The evaluation of negative conversion of total metabolic tumor volume (TMTV) by PET/CT after treatment does not really reflect the process of tumor metabolism [6,7]. Although PI3K inhibitor as idelalisib is approved for refractory FL, but it demonstrates limited effects on patients with POD24 [8]. Immunotherapies such as CD47 mAb [9,10], PD-1 mAb [11,12], and immunomodulatory lenalidomide, are declared unsatisfactory responses in cases of relapsed FL [13,14].

Increased evidences confirmed that changes in tumor cell metabolism can affect a variety of immunocytes in tumor microenvironment (TME) which also could in turn affect the survival and growth of tumor cells [15]. Aerobic glycolysis is the main metabolic pathway of tumor cells, and glycolysis-mediated metabolic remodeling occurs in tumor cells and various immunocytes in TME [16]. Lactate accumulation, as the most important vehicle, derived from excessive glucose consumption promotes tumor growth through restraining nuclear factor of activated T cells, diminishing interferon-γ levels and suppressing tumor immunosurverillance [17]. Glucose transport protein 1 (GLUT1) exists in a variety of tissue cells, and its function is to assist glucose transport into the cell. In a large number of studies, it has been confirmed that GLUT1 is highly expressed in tumors, mediating increased glucose uptake by tumor cells and promoting tumor growth by enhancing glycolysis of TME [15,18]. However, its expression characteristics and its specific mechanism of action in FL remain unclear.

Previous study found that GLUT1 expression was higher in relapsed FL [19], Here, we aimed to explore the molecular mechanism that GLUT1-mediated metabolic remodeling influences immunocytes in the TME and how it further affected tumor growth and the occurrence of POD24 in FL.

Materials and methods

Samples

Pre-treatment samples of FL patients with POD24 (n=34) and FL patients with long-term survival (n=30, more than 10 years) from January 1998 to January 2020 treated in the Harbin Medical University Cancer Hospital were retrieved. The patients who died within 24 months after initial treatments were excluded due to the unavailable evaluation of the POD24 events. All samples were confirmed FL diagnosis without histological transformation after rigorous pathological examinations. The Institutional Review Board (IRB) of this institution granted approval for the research protocol and procedures. All participants signed the consent forms before participating. POD24 was defined as relapse within 24 months of frontline initial chemoimmunotherapy [3]. The baseline clinical characteristics are displayed in Table 1.

Immunohistochemical staining (IHC)

Sample slides staining was performed as manufacturer's instructions. The antibodies included the anti-GLUT1 (2A5A2, Proteintech), anti-CD206 (2A6A10, Proteintech), and anti-CD8 (1G2B10, Proteintech). The intensity of GLUT1 staining was quantified using the *H*-score methods as [$\sum$ (3 × percent of cells with strong staining + 2 × percent of cells with moderate staining + 1 × percent of cells with weak staining)]. The quantification of CD206 and CD8 was calculated the percent of positive cells within 3 different fields.

Table 1
Initial characteristics of 64 patients with follicular lymphoma.

Parameters	POD24 (34) *n* (%)	Long-term remission (30) *n* (%)
Median age (range)	62.0 years (46.0-79.0)	60.5 years (45-67.0)
Gender		
female	15 (44.1)	14 (46.7)
male	19 (55.9)	16 (53.3)
B symptoms		
no	26 (76.5)	22 (73.3)
yes	8 (23.5)	8 (26.7)
ECOG		
0-1	32 (94.1)	30 (100)
≥2	2 (5.9)	0 (0)
Elevated LDH		
No	25 (73.5)	26 (86.7)
Yes	9 (26.5)	4 (13.3)
Hemoglobin		
≥12 g/dL	27 (79.4)	27 (90.0)
<12 g/dL	7 (20.6)	3 (10.0)
Stage		
I/II	3 (8.8)	5 (16.7)
III/IV	31 (91.2)	25 (83.3)
Number of nodal sites		
≤4	22 (64.7)	26 (86.7)
>4	12 (35.3)	4 (13.3)
FLIPI score		
low	4 (11.7)	7 (23.3)
intermediate	13 (38.2)	12 (40.0)
high	17 (50.0)	11 (36.7)
Histology		
1-2	20 (58.8)	20 (66.7)
3a	11 (32.4)	8 (26.7)
3b	3 (8.8)	2 (6.7)
Chemoimmunotherapy regimen		
R-CHOP[a]	24 (70.6)	26 (86.7)
R-COP[b]	9 (26.5)	3 (10.0)
R-FC[c]	1 (2.9)	0 (0)
Others[d]	0 (0)	1 (3.3)

*Abbreviation: FL, follicular lymphoma; POD24, progression of disease within 24 months; ECOG, Eastern Cooperative Oncology Group; LDH, lactate dehydrogenase; FLIPI, FL International Lymphoma Prognostic Index.
[a] R-CHOP, cyclophosphamide, doxorubicin, vincristine and prednisolone plus rituximab
[b] R-COP, cyclophosphamide, vincristine and prednisolone plus rituximab
[c] R-FC,fludarabine, and cyclophosphamide plus rituximab
[d] Others, rituximab-lenalidomide, rituximab-Bendamustine, and watchful waiting.

Macrophage, exhausted CD8+ T cells, Tregs inductions and co-culture

The initial macrophages (MΦ) were induced as previous from PBMCs [20] and re-stimulated with IL-4 and IFNγ (Supplementary Fig. S1). The purified CD8+ T by magnetic beads [21] were cultured with CD3/CD28 activators, IL-2 and PD-L1 Fc Chimera for the exhausted T cells, and were stimulated by pre-coated anti-CD3 and soluble anti-CD28 for effector T cells. Human naive CD4+ T cells from PBMC were induced with anti-CD3, anti-CD28 and IL2 for Tregs which were purified by flow cytometry [22].

WSU-FSCCL and DOHH2 were obtained from the Fudan IBS Cell Resource Center (FDCC, China). The Mϕ cells were co-cultured with the FL cells (ratio 1:3) or with the supernatant. FL cells were co-cultured with M2 TAM, exhausted CTL and Tregs at a 1:3 tumor:immunocytes ratio.

Cell transfection and lactate detection

GLUT1 siRNA were synthesised by GenePharma (Shanghai, China). The GLUT1 overexpression and non-sense plasmids were constructed by GeneCopoeia (Shanghai, China). DOHH2 were transfected with GLUT1 over-expression plasmid or GLUT1 siRNA and their non-sense controls using Lipofectamine 2000 reagent (Invitrogen, USA) according to the manufacturer's protocol [23]. Lactate production in DoHH2-GLUT1, DoHH2/siRNA GLUT1 and DOHH2-Control were detected using LA assay kit (Solarbio® BC2230) according to the manufacturers.

Flow cytometry

FlowJo software (Tree Star) were used with antibodies (Biolegend) of APC-CD8, PE-PD1, APC-CD4, APC/Cyanine7-CD25, anti-FITC-CD206, PE-CD68, Alexa Fluor® 488-TNF-α, APC/Cy7-IFN-γ, anti-PE-Foxp3, and PE/Cy7-IL-10. M2-like macrophages were identified by CD68+ and CD206+. The exhausted T cells was defined as CD8+ PD-1Hi/IL-10Hi/TNF-α Lo/IFN-γ Lo. Tregs were represented with the expression ratio of Foxp3 in CD25+CD4+ T cells.

Western blotting

Extractions were separated on SDS–polyacrylamide gels. Primary antibodies (Proteintech) included mTOR, p-mTOR-S2448, AKT, pAKT (Ser473), PI3K (P85), pPI3K (P85) (Y467/Y199/Y464), GLUT1 and β-actin (ZSGB-BIO). The images were captured using the ChemiDocTM CRS + Molecular Imager (Bio-Rad) and analyzed by Image J software.

Multiplexed ion beam imaging by time of flight (MIBI-TOF)

Paraffin-embedded tissue slides were stained using the primary antibodies with metal-conjugation by the Maxpar labeling kit (Fluidigm) based on Biotek (Berten Instruments) (Supplementary Table S1). Imaging mass cytometry (IMC) Images were captured by MIBI-TOF Imaging System (Fluidigm). MCDViewer, CellProfilor, and HistoCAT were processed for successful image captures. The data were segmented into single cells by Cellprofiler v3.1.8. The single-cell markers were measured by histoCat v1.75 with *z*-scored means. Twenty defined clusters were assigned (Euclidean distance and Ward's linkage) according to their mean pertinence of related markers. The uncertainty of each subtree was assessed by multiscale bootstrap resampling (R package pvclust, v.2.0). Single-cell data with a high dimension was degraded into two dimensions by the nonlinear dimensionality reduction algorithm (t-SNE). The pairwise neighbor interactions for cell type significance were detected using Cellprofier Measure Object Neighbors module and neighborhood (https://github.com/BodenmillerGroup/neighbouRhood) with permutation-test-based analysis of the spatial distribution. Four pixels (4 μm) showed the boundary of neighboring cells. $p < 0.01$ were identified as significance.

Tandem mass tag peptide (TMT) labeling proteomics

TMT® Mass Tagging Kits and Reagents (Thermo) were applied for TMT labeling of the peptides with lysed (Sigma) sample. The tissues were fractionated and shotgun proteomics analyzes were performed by EASY-nLCTM 1200 ultra-high-pressure liquid chromatography system (Thermo Fisher) with Q Exactive HF (X) mass spectrometer (Thermo Fisher) operated in the data-dependent acquisition (DDA) mode. The final spectra of each run were hunted solely according to the homo_sapiens_uniprot_2020_7_2.fasta (192320 sequences) database by using the search software Proteome Discoverer 2.2 (PD 2.2, Thermo). The differentially expressed proteins (DEP) were defined as fold change (FC) ≥ 1.2 and p-value ≤ 0.05 for the upregulated proteins and FC ≤ 0.83 and p-value ≤ 0.05 for the downregulated proteins using t-test. Gene Ontology (GO), Clusters of Orthologous Groups (COG) and Kyoto Encyclopedia of Genes and Genomes (KEGG) and InterPro (IPR) functional analysis were carried out with the non-redundant protein database (Pfam, PRINTS, etc.). The STRING-db server (http://string.embl.de/) was used to predict the probable interprotein interactions.

Statistics

Statistical analyzes were performed by SPSS version 25.0.0 (IBM Corporation, Armonk, NY, USA), R software (version 3.5.1), and The GraphPad Prism (version 9; San Diego, USA). The random forest classifier was applied for proximity relations of categorical immunophenotype to train the model. The pre-processed data set was split into training set and validation set. The 5-fold trainings cross validation were used to prevent overfitting. Receiver operating characteristic (ROC) curve was conducted to assess the random forest classifier with comparing the area under the curve (AUC). Association analysis was investigated with the χ^2 test. The student's *t*-test was used for a single comparison between two groups. The one-way analysis of variance (ANOVA) was employed for multiple groups comparisons. Three independent repeats were executed to exclude the outliers by ROUT methods. Data were shown as mean ± SEM. Boxplots was visualized with values ranging from 10 to 90%. $p < 0.05$ is considered as statistical significance. * $p < 0.05$, ** $p < 0.01$, *** $p < 0.001$, and **** $p < 0.0001$.

Results

Clinical correlation of GLUT1 expression and tumor-infiltrating immunocytes

IHC analysis were performed between tumors from patients with long-term remission and patients with POD24, who were at the similar stage, with parallel age, semblable histological grade and analogical treatments. Baseline tumor from patients with POD24 had a higher proportion of GLUT1 overexpression (Fig. 1A, $p < 0.01$), more M2-type TAMs (Fig. 1B, $p < 0.001$) and CD8+ T cells (Fig. 1C, $p < 0.01$) infiltrations. We identified the GLUT1-low group (n=27) and the GLUT1-high group (n=37) based on IHC scores. We found that the expression of GLUT1 had no significant difference among stratified groups of age, gender, B symptom, ECOG performance, LDH level, hemoglobin, clinical stage, number of nodal sites and histological grade. However, the high expression of GLUT1 was correlated with high FLIPI scoring (P=0.007). Besides, the high expression of GLUT1 was positively associated with high density of M2-like macrophage (P=0.037) and CD8+ T cells (P=0.021) (Supplementary Table S2). Furthermore, whether the effective or exhausted CD8+ T cells were specifically identified as follows.

Elevated GLUT1 level and relatively inhibitory TME in FL with POD24

TAM and exhausted T cells link to poor survival in lymphoma [24–26]. We spatially expanded illustrations of spatial immunocytes comprehensively and intuitively using phenotype panels by IMC. In baseline tumor from patients with POD24, myeloid and lymphatic cells shared a similar ratio among large CD45+ immunocytes. Scattered CD8+ and CD4+ T cells with closer proportions were dominated with adjacent space. The CD8+, PD-1+ and Tim-3+ CTL bordered on tumor PD-L1, implying PD-1/PD-L1 axis-mediated T cell dysfunction. Most FOXP3+ Tregs and sectional CD25-non-regulatory T helper cells bifurcated from CD4+ T cells indicated attenuated antitumor status. Despite that CD14+CD68+ or partial CD11c+ macrophages linked to the effective status, the weak level of CD16 implied relative immune-incapability. In stark contrast, the long-term remission baseline tumors presented extreme amounts of CD45+ immune cells with close proximity. Vast clustered PD-1+ CTL (median level) with functional pattern were closer to the tumor cells. Minor FOXP3+ Tregs and more Bcl-6+ follicular T helper cells (Tfh) shared major frequency within CD4+ T cells. Non-regulatory CD25+, PD-1hi, CD4+ T cells were far

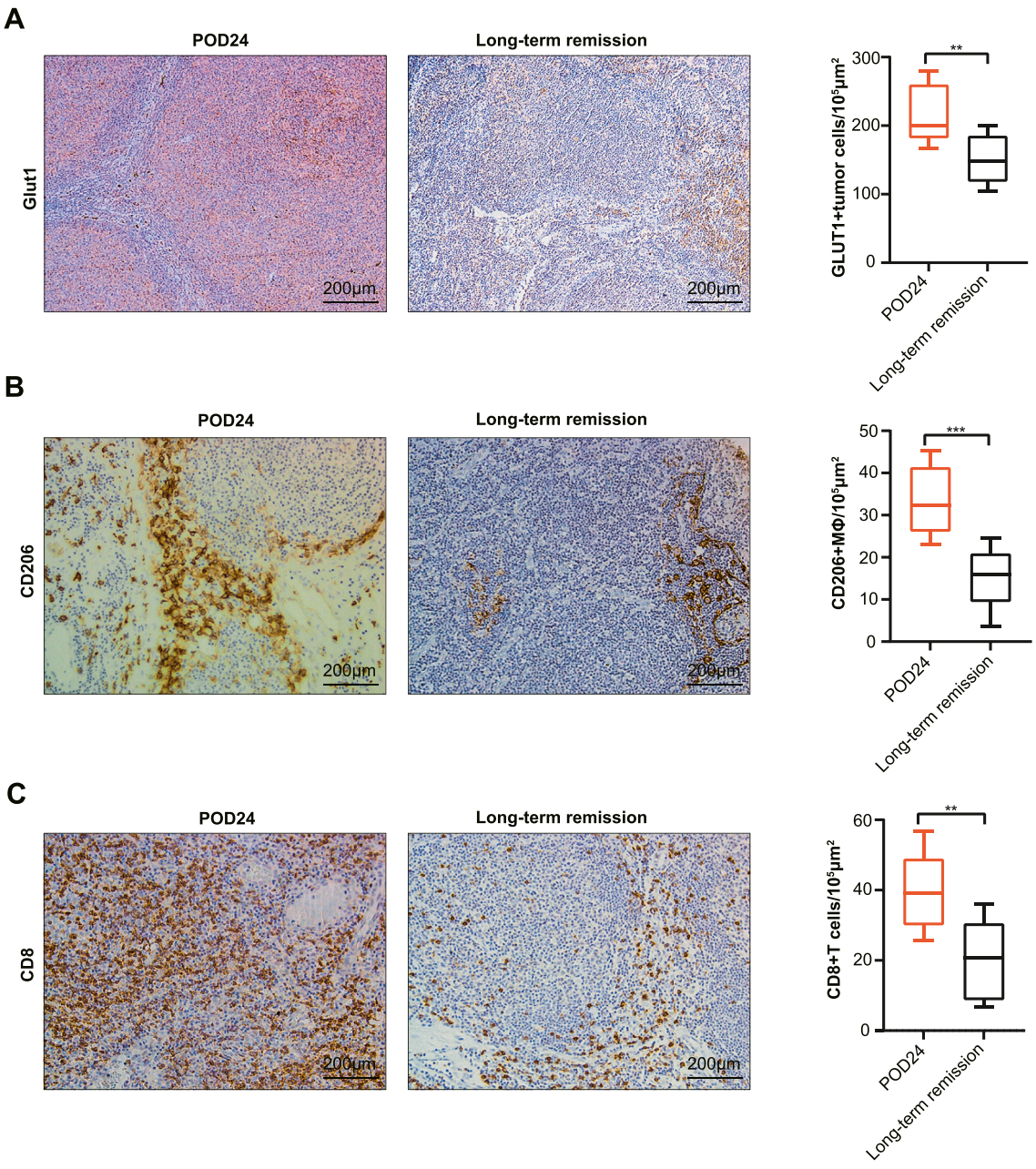

Fig. 1. FL with POD24 showed higher expression of GLUT1 and more M2-like TAM and CD8+ T cells. Representative staining and H-score assessment of GLUT1 (A), CD206 (B) and CD8 (C) in FL with POD24 and with long-term remission. Magnification × 100. Scale bar: 200μm. Data are presented as mean ± SEM. *P<0.05, **P<0.01; ***P<0.001; ****P<0.0001. GLUT1, Glucose transporter 1; TAM, tumor associated macrophages.

away from tumor cells. A higher proportion of macrophages with CD14+CD68+ and major CD11c+CD11b+ phenotypes associated with effective M1-like phenotype were close to tumor center. In addition, a higher ratio of CD19+Bcl-6+ tumor cells were correlated to increasing PD-L1 expression in FL with POD24, while Bcl-6+CD19- non-tumor B cells occupied a major cluster with less PD-L1 expression in long-term remission FL (Fig. 2 and Supplementary Fig. S2). Referring to 20 normalized immunocytes communities (Fig. 3A), compared with long-term remission ones, baseline tumor from FL with POD24 exhibited more clusters with immunosuppressive phenotypes (Fig. 3B). This immunophenotypes were obviously clustered (Fig. 3C) and neighbouring analysis estimated that the lower proportions of functional immunoctyes had features as farther spatial distance, such as S19 for Th cells and S6 for M1-like macrophages (Fig. 3D–F). These may indicate the decrease of anti-tumor immunity. By analyzing immunophenotypes of spatial immunocytes (panels in Supplementary Table S1), these different expressions and neighbouring relationship (n=69) could specifically distinguish the two groups (AUC=1.0). These typical immunophenotypes such as TGF-β, PD-1, and neighbour cells (n=48), could be applied to identify FL with POD24 (Fig. 3G-H).

Next, we further explored the differences of immunophenotypes from functional levels in baseline tumors. We totally identified 2193 common proteins with reliable quality control (Supplementary Fig. S3). Compared to the FL with long-term remission, in FL with POD24, the differential protein clustering portrayed increased expression GLUT1 (p = 0.017) and immunosuppressive markers such as PD-1, PD-L1, CD206, CD163, IL-10, TGF-β, and related chemokines, such as CCL17, CCL22, CCL5, and CXCL5. Conversely, the expression of inflammatory cytokines such as TNF-α, IFN-γ, and IL-12 decreased (Fig. 4A, B). Simultaneously, in FL with POD24, the T and B cell receptor signaling pathways (p =

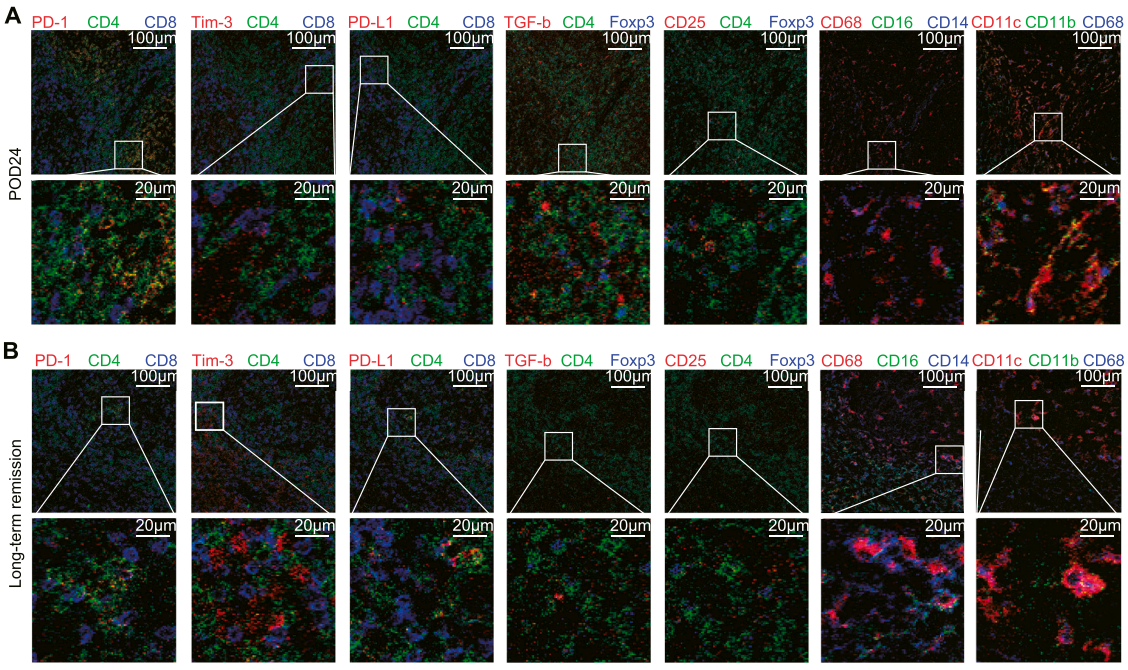

Fig. 2. The different spatial distributions of typical immunocytes between FL with POD24 and long-term remission. Upward side, 500 μm × 500 μm, scale bar: 100 μm; Downward side, 100 μm × 100 μm, scale bar: 20 μm. TIME, tumor immunomicroenvironment; FL, follicular lymphoma.

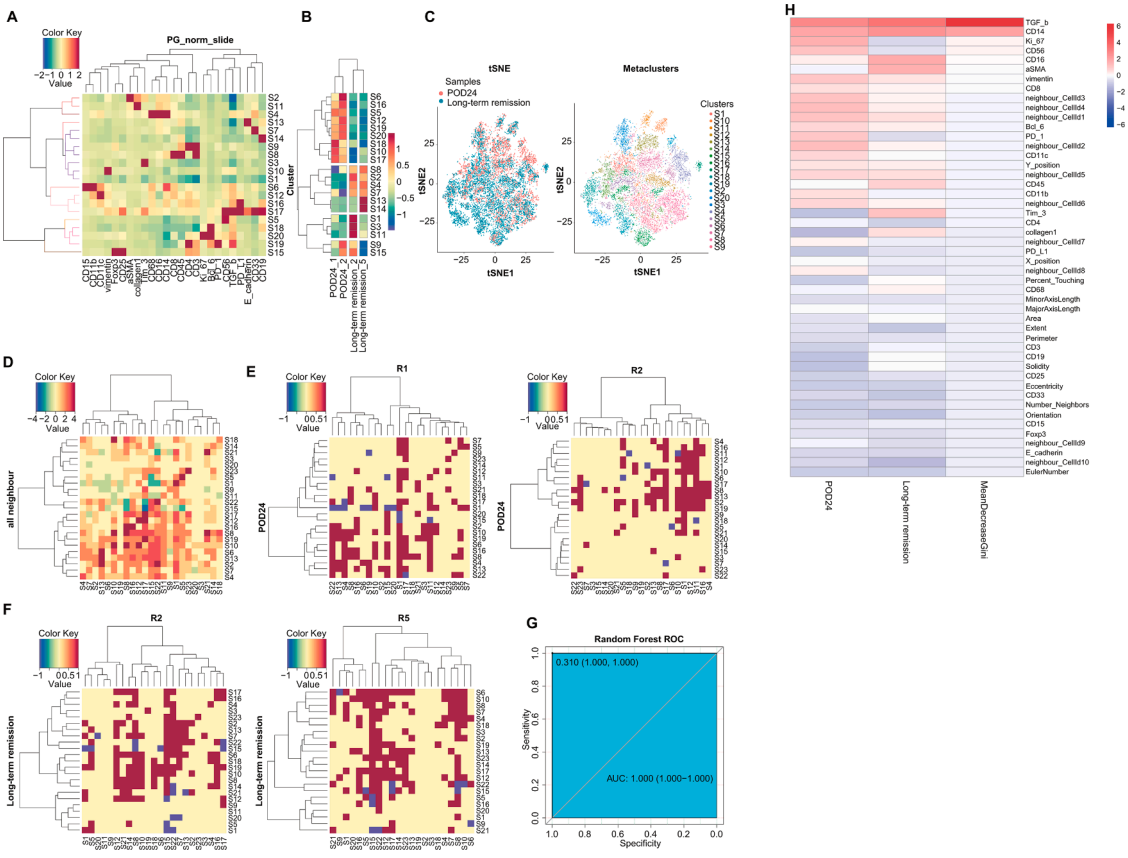

Fig. 3. Neighbor correlation analysis of spatial immunocytes and prognostic classifier model. (A) Tumor cells and immunocytes in TME from all regions were standardly clustered by protein expression markers (total S20). (B) The different expression values of 20 resulting clusters (y axis) between FL with POD24 and long-term remission (x axis) is shown, scaled from -1 to 1. (C) tSNE embedding for Tumor cells and immunocytes in TIME. Cells are colored by either sample as in (left) or cluster (right). Heatmaps denote spatial proximity *z* scores between pairs of clusters in regions of all neighbours (D), in tumor regions of R1 and R2 of FL with POD24 (E) as well as R2 and R5 of FL with long-term remission (F), from different patients. (G) The random forest classifier assessed by Receiver operating characteristic (ROC) curve with the area under the curve (AUC) based on immunophenotypes. (H) Heatmaps character the quantified spatial distinction of immunophenotypes between two groups. TME, tumor microenvironment; R, roi.

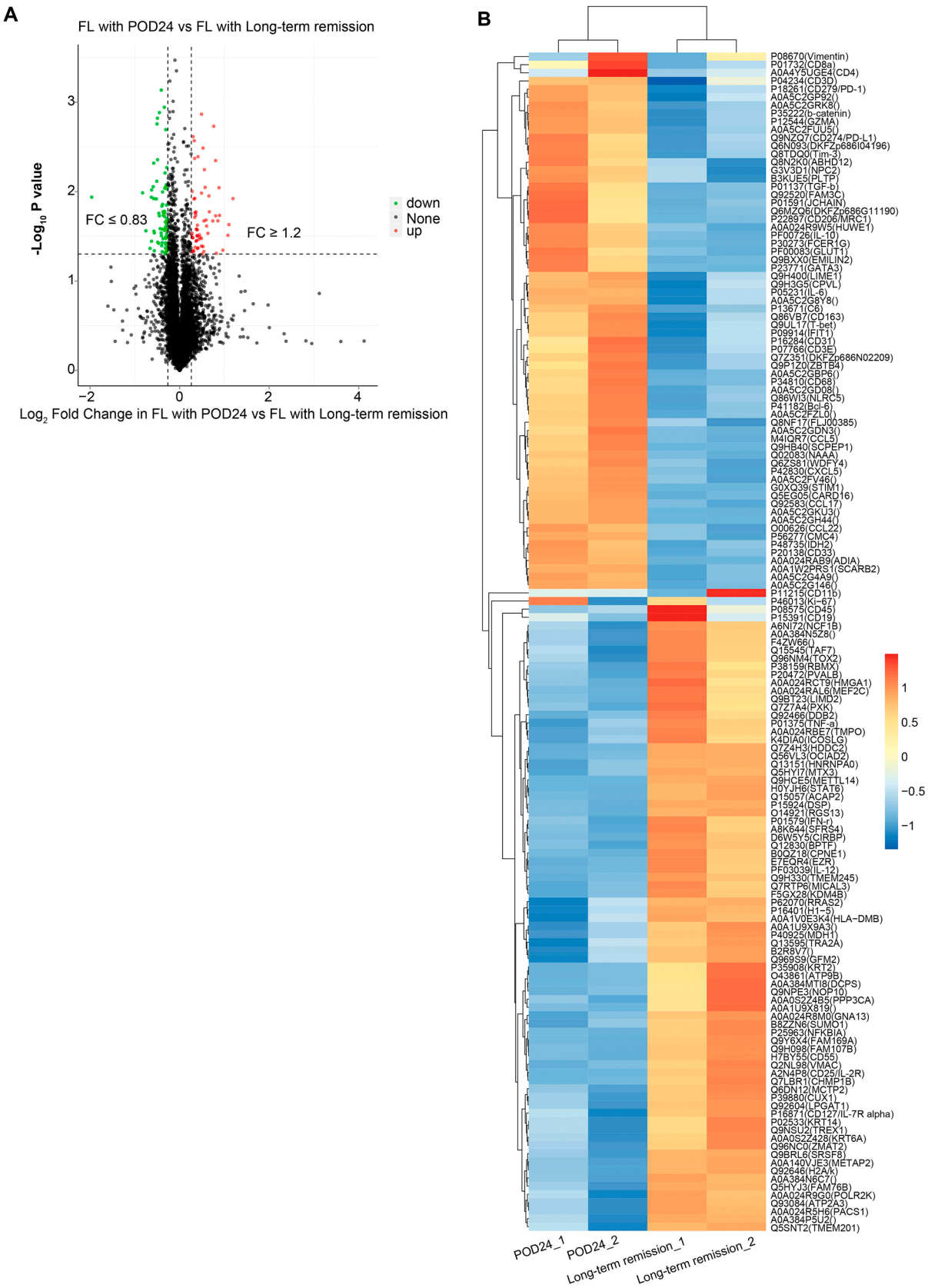

Fig. 4. Increased immunosuppressive proteins and GLUT1 in FL with POD24 compared to FL with long-term remission. (A) Volcano map suggested the different proteins. The x-axis specifies the fold-changes (FC) and the y-axis specifies the negative logarithm to the base 10 of the unpaired t-test *p*-values. Vertical and horizontal lines reflect the filtering criteria (FC $\geq$ 1.2 and *P*-value $\leq$ 0.05 for up-regulated proteins, FC $\leq$ 0.83 and *P*-value $\leq$ 0.05 for down-regulated proteins). Red and green dots represent probe sets for protein expressed at significantly higher (60) and lower (75) levels. (B) Specific up and down regulated immuno-related proteins and GLUT1 protein ($p = 0.017$) depicted by Heatmap. n=4 samples. *P*-value $\leq$ 0.05 was statistically significant with unpaired t test.

0.01, $p = 0.005$) associated with PD-1/PD-L1 interaction (Supplementary Fig. S4A) were upregulated, but no significant difference in activation of PI3K/ Akt /mTOR signaling pathway was detected between the two groups ($p = 0.083$) (Supplementary Fig. S4B). Distinct subcellular localization and interaction network within differential proteins implied their differently contributed influence to TME (Supplementary Figs. S4C and S5). Accordingly, FL with different prognosis had different TME contexture as well as GLUT1 level, potentially relating to occurrence of POD24 event.

GLUT1 mediates tumor glycolysis and affects M2-like macrophages polarization

We next focused on whether tumor-driving functional alteration in immunocytes was associated with GLUT1-mediated tumor glycolysis. We explored the M2-type polarization of macrophages after co-culturing with tumor cells of GLUT1 overexpression (DOHH2-GLUT1) and GLUT1 knock-down (DOHH2/siRNA GLUT1). Firstly, lactate accumulation in DOHH2-GLUT1 cell medium was significantly higher than DOHH2/siRNA GLUT1 (Fig. 5A), demonstrating GLUT1 could enhance glycolysis of FL. Moreover, the supernatant of DOHH2-GLUT1 culture medium could induce more M0 macrophages changing into CD206+ M2-type macrophages, and the proportion of induced M2-type TAMs decreased after intervention with GLUT1 knock-down (DOHH2/siRNA GLUT1, Fig. 5B-C, $p < 0.001$). Collectively, FL cells could induce M2-like macrophages, associated with the glycolysis mediated by GLUT1.

GLUT1-high FL could be triggered the overactive PI3K/AKT/mTOR signaling

We characterized that FL with POD24 had higher proportion of TGF-β, PD-1, and PD-L1. Indeed, they had capability to activate tumor growth pathways [27–30]. Accordingly, we performed cytokines stimulation to construct human-derived M2-like macrophages, showing CD68+CD206+ phenotypes of 99.2% (Supplementary Fig. 6A). The efficient induction of Foxp3+ Tregs were achieved of 2.4% (Supplementary Fig. 6B), which was more noteworthy exceeding previous report (0.48%) [22]. Exhausted T cells were acquired and defined as PD-1hiIL-10hiTNF-αloIFN-γlo (Supplementary Fig. S6C-D; $p < 0.001$). In order to be close to clinical setting, we used tumor cell lines from different disease stages with the distinct expression of GLUT1. The DOHH2 cell line derived from refractory FL [31] showed high-expressed GLUT1 in contrast to that in WSU-FSCCL cell line annotated to low-grade FL [32] (Fig. 6A).We reconstructed resembling TME by co-cultured system and detected that the WSU-FSCCL cells (low GLUT1 level) failed to activate tumor PI3K, Akt, and mTOR proteins. In

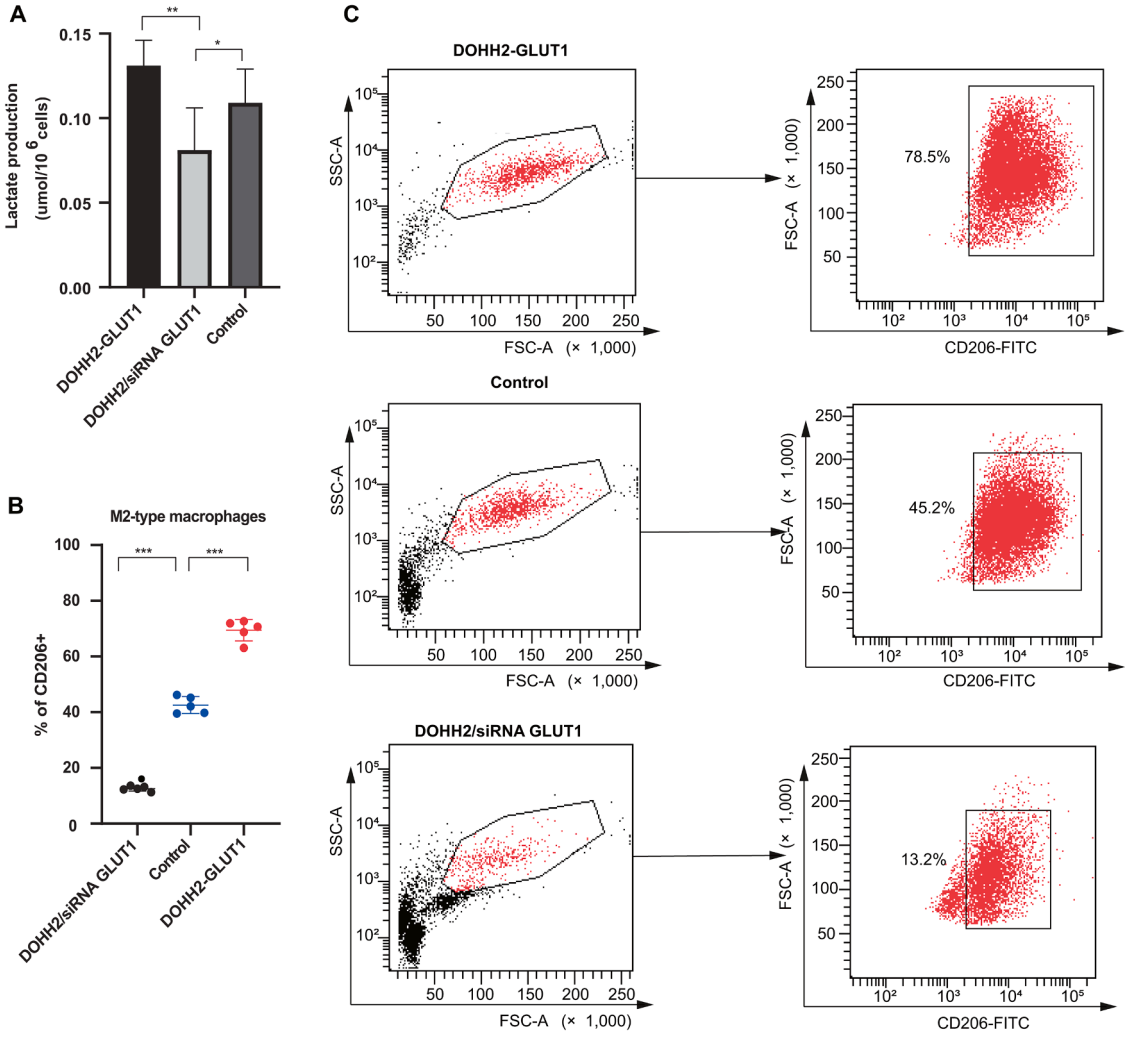

Fig. 5. GLUT1 mediated lactate production which may induce macrophage to M2 polarization. (A) The lactate content in the medium of DOHH2-GLUT1 and DOHH2/siRNA GLUT1 cells. (B) Flow cytometry analysis of M2 surface marker CD206 from all macrophage co-cultured with DOHH2-GLUT1 and DOHH2/siRNA GLUT1 cells. All experiments were five times biological replicates. Data are presented as mean ± SEM. Statistical analyzes by Ordinary one-way ANOVA, Tukey's multiple comparisons test. *P<0.05, **$P < 0.01$; ***P<0.001; ****P<0.0001.

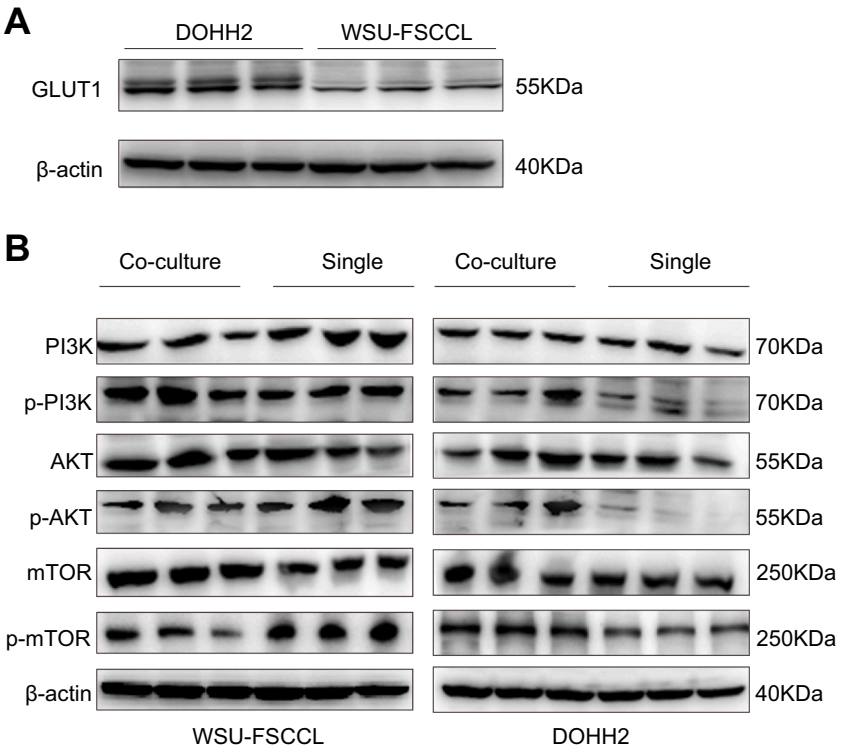

Fig. 6. The activation of PI3K/AKT/mTOR signaling in different FL cells surrounded by suppressive immunocytes was distinct. (A) Different GLUT1 protein expression levels between WSU-FSCCL and DOHH2 cells. (B) Expression of PI3K, AKT, mTOR, p-PI3K, p-AKT and p-mTOR were detected following co-cultured with M2 TAM, exhausted T cells and Treg cells in WSU-FSCCL and DOHH2 cells. β-actin was used as a loading control. Three biologically independent samples for each group. Single, only cancer cells; Co-culture, cancer cells co-cultured with M2 TAM, exhausted T cells and Treg cells. GLUT1, Glucose transporter 1; TAM, tumor associated macrophages; Treg, regulatory T cells. TME, tumor microenvironment.

contrast, DOHH2 cells (high GLUT1 level) achieved activation (Fig. 6B). Interestingly, inhibitory TME may over activate tumor growth signaling, potentially associated with the expression of GLUT1.

Discussion

Recent study disclosed that due to the number advantages of B cells in FL, the relative contribution of intratumoral T cells to TMTV was limited, as proved that CD4+ Tfh and activated CD8+ T cells were clonally expanded in low TMTV status compared to those with a high TMTV. Pretherapy TMTV based on 18F-fluorodeoxyglucose uptake best reflects the malignant B-cell burden and maximum standardized uptake value (SUVmax) was influenced by intratumoral T cells [33]. However, these two parameters always present the inconsistent trend and could not reflect the complete metabolic process of tumor. Metabolic remodeling is essential and bidirectional between tumor cells and immunocytes, especially glycolysis [34]. GLUT1 protein associated with glycolysis metabolism [15,18] were identified in FL with POD24 both by previous study [19], and our results exactly proved the increase of GLUT1 in FL with POD24 compared to FL with long-term remission after balancing other influenced factors. We also found that expression of GLUT1 had no statistical difference among multiple clinical parameters but its high expression was associated with high FLIPI scoring, which exactly proved GLUT1 should be a key factor of disease biology.

Tumor-imposed nutrient restrictions can lead to hyporesponsiveness of immunocytes, even when the tumors are highly antigenic [9]. We demonstrated that FL cell with high expression of GLUT1 had anaerobic glycolysis measured by lactate accumulation and the ability to induce more M2-like macrophages. Besides, increased expression of GLUT1 was significantly associated with the greater frequency of M2-type macrophages and CD8+ T cells. But there remained lacking identification of functional phenotypes in CD8+ T cells (effective or exhausted). Comprehensive spatial distribution analysis settled with this problem and further showed the spatial features. There were more scattered clusters comprised of suppressive immunocytes far away from tumor center, such as PD-1+TIM-3+ T cells, FOXP3+ Tregs, and CD11c+ mature DC, in TME of FL with POD24. They spatially connected to PD-L1, implying tumor immune escape. Some epithelial-mesenchymal transitions (EMT)-derived protein as a-SMA exerted short and long-range effects on tumor invasiveness. A minor scale of anti-tumor CD11c+CD11b+ M1-like macrophages and BCL-6+ Tfh contributed to curtail effective anti-tumor immunity. Farther spatial distances between 20 differentiated functional immunocytes in FL with POD24 indicated impaired anti-tumor immune reaction. These spatial features indicated the changes of TME brought from tumor with distinct GLUT1 level. We also provided a good classifier using these spatial signatures of immunophenotypes to distinguish the tumor with POD24 and long-term remission, indicating the prognostic value of spatial distribution in TME.

The dysfunction of immunocytes is involved in diverse signaling pathways such as PI3K-Akt-mTORC1/C2, REDD1/mTOR, and CPT1A/FAO, all associated with GLUT1-related glycolipid transformation [35–37]. In turn, pro-tumor immunocytes could facilitate tumor growth signaling pathway for tumor cells such as canonical PI3K/Akt/mTOR [30]. For example, PD-L1/PD-1 interaction between tumor and suppressive T cells affects tumor Akt/mTOR signaling [27]. TAM-derived collagen fosters tumor α2β1/PI3K/Akt signaling and TGF-β promotes tumor PI3K/Akt/mTOR pathways [28–30]. Meaningfully, we detected greater accumulation of TGF-β, PD-1, and PD-L1 in FL with POD24 than that in long-term remission ones. Moreover, *in vitro*, under the durative influence of suppressive immunocytes, GLUT1-high FL cells could activate PI3K/AKT/mTOR signaling. It seems paradoxical for miss of tracking the overactive PI3K/AKT/mTOR signaling in both FL tissues with POD24 and long-term remission by proteomics. Indeed, it exactly indicated that FL might depend on GLUT1 to support self-progression in POD24 stage and gradually activate tumor growth pathways in the later stage. Generally, this observation illustrated the potential role of GLUT1 expressions to link tumor cells and its TME, and the association with POD24 event.

Durable suppressive TME could affect tumor-intrinsic PI3K or other metabolism pathways (c-MYC, MAPK) [38,39] following the disease progression. Furthermore, PI3K inhibitor may not only target tumor cells but also the T cells toward aggravating immune dysfunction [40].

FL with POD24 has high expression of GLUT1 and showed the potential relationship with TME. These observations provided an interpretation for the limited responses of PI3K inhibitors in FL with POD24 [41] and significant guidance for future treatment based on GLUT1. At present, metformin, an antimetabolit, has been confirmed to inhibit PPARδ agonist-mediated tumor growth, aiming to GLUT1 target [42]. The universality to acquisition of metformin provides an insight to the powerful clinical antimetabolit therapy for FL with POD24, which can be generalized in future researches.

Taken together, our study represented an important step in further understanding of the potential role of GLUT1-triggered abnormal metabolism in FL with POD24. Identifying the potential crosstalk between GLUT1 and TME may benefit FL with POD24 from early anti-metabolism therapy and immunotherapy in the future.

Conclusion

In summary, increased GLUT1 expression was found in baseline tumor from FL patients with POD24. Tumor cells overexpressing GLUT1 could domesticate immunocytes to form an immunosuppressive TME, which promotes the occurrence of POD24 and gradually activates PI3K/Akt /mTOR pathway of tumor cells in the later stage.

Data availability statement

All data in this study are available from the lead contact with a completed Materials Transfer Agreement. The mass spectrometry proteomics data are available via ProteomeXchange with identifier PXD031257. Reviewer account details: Username: reviewer_pxd031257@ebi.ac.uk Password: HLNIMzUY

Ethics approval and consent to participate

All study procedures were approved by the Institutional Review Board (IRB) of the Cancer Hospital of Harbin Medical University. All participating patients provided their written informed consent. This study was performed in concordance with the Declaration of Helsinki.

Patient consent

Written informed consent was obtained from the parents.

Consent for publication

The authors affirm that human research participants provided informed consent for publication of clinical data in tables and figures.

Funding

This work was supported by the major project of National Natural Science Foundation of China. No. 81730074 and N10 project in the Harbin Medical University Cancer Hospital.

CRediT authorship contribution statement

Yuwei Deng: Formal analysis, Writing – original draft. **Jianli Ma:** Formal analysis, Writing – original draft. **Shu Zhao:** Data curation. **Ming Yang:** Data curation. **Yutian Sun:** Data curation. **Qingyuan Zhang:** Supervision, Data curation, Writing – original draft.

Declaration of Competing Interest

The authors have no relevant financial or non-financial interests to disclose.

Acknowledgments

Harbin Xingyun Medical Inspection Institute Co. Ltd and Beijing Jinkorui Medical Laboratory provided technical assistance. The clinical data collection was supported by the Cancer Hospital of Harbin Medical University.

Supplementary materials

Supplementary material associated with this article can be found, in the online version, at doi:10.1016/j.tranon.2022.101614.

References

[1] A. Carbone, S. Roulland, A. Gloghini, et al., Follicular lymphoma, Nat. Rev. Dis. Prim. 5 (1) (2019) 83, https://doi.org/10.1038/s41572-019-0132-x [published Online First: 2019/12/14].
[2] S. Guo, J.K. Chan, J. Iqbal, et al., EZH2 mutations in follicular lymphoma from different ethnic groups and associated gene expression alterations, Clin. Cancer Res. 20 (12) (2014) 3078–3086, https://doi.org/10.1158/1078-0432.CCR-13-1597 [published Online First: 2014/03/19].
[3] C. Casulo, P.M. Barr, How I treat early-relapsing follicular lymphoma, Blood 133 (14) (2019) 1540–1547, https://doi.org/10.1182/blood-2018-08-822148 [published Online First: 2019/02/01].
[4] C. Casulo, M. Byrtek, K.L. Dawson, et al., Early relapse of follicular lymphoma after rituximab plus cyclophosphamide, doxorubicin, vincristine, and prednisone defines patients at high risk for death: an analysis from the national LymphoCare study, J. Clin. Oncol. 33 (23) (2015) 2516–2522, https://doi.org/10.1200/JCO.2014.59.7534 [published Online First: 2015/07/01].
[5] A. Freedman, E. Jacobsen, Follicular lymphoma: 2020 update on diagnosis and management, Am. J. Hematol. 95 (3) (2020) 316–327, https://doi.org/10.1002/ajh.25696 [published Online First: 2019/12/10].
[6] A. Pastore, V. Jurinovic, R. Kridel, et al., Integration of gene mutations in risk prognostication for patients receiving first-line immunochemotherapy for follicular lymphoma: a retrospective analysis of a prospective clinical trial and validation in a population-based registry, Lancet Oncol. 16 (9) (2015) 1111–1122, https://doi.org/10.1016/S1470-2045(15)00169-2 [published Online First: 2015/08/11].
[7] A. Gallamini, A. Borra, FDG-PET scan: a new paradigm for follicular lymphoma management, Med. J. Hematol. Infect. Dis. 9 (1) (2017), e2017029, https://doi.org/10.4084/MJHID.2017.029 [published Online First: 2017/05/18].
[8] J.P. Leonard, M. Trneny, K. Izutsu, et al., AUGMENT: a phase iii study of lenalidomide plus rituximab versus placebo plus rituximab in relapsed or refractory indolent Lymphoma, J. Clin. Oncol. 37 (14) (2019) 1188–1199, https://doi.org/10.1200/JCO.19.00010 [published Online First: 2019/03/22].
[9] M. Yang, D. McKay, J.W. Pollard, et al., Diverse functions of macrophages in different tumor microenvironments, Cancer Res. 78 (19) (2018) 5492–5503, https://doi.org/10.1158/0008-5472.CAN-18-1367 [published Online First: 2018/09/13].
[10] C. Liu, M. Chikina, R. Deshpande, et al., Treg cells promote the srebp1-dependent metabolic fitness of tumor-promoting macrophages via repression of CD8(+) T Cell-derived interferon-gamma, Immunity 51 (2) (2019) 381–397, https://doi.org/10.1016/j.immuni.2019.06.017, e6[published Online First: 2019/07/28].
[11] B.C. Miller, D.R. Sen, R. Al Abosy, et al., Subsets of exhausted CD8(+) T cells differentially mediate tumor control and respond to checkpoint blockade, Nat. Immunol. 20 (3) (2019) 326–336, https://doi.org/10.1038/s41590-019-0312-6 [published Online First: 2019/02/20].
[12] E. Dodagatta-Marri, D.S. Meyer, M.Q. Reeves, et al., alpha-PD-1 therapy elevates Treg/Th balance and increases tumor cell pSmad3 that are both targeted by alpha-TGFbeta antibody to promote durable rejection and immunity in squamous cell carcinomas, J. Immunother. Cancer 7 (1) (2019) 62, https://doi.org/10.1186/s40425-018-0493-9 [published Online First: 2019/03/06].
[13] B. Farhood, M. Najafi, K. Mortezaee, CD8(+) cytotoxic T lymphocytes in cancer immunotherapy: a review, J. Cell Physiol. 234 (6) (2019) 8509–8521, https://doi.org/10.1002/jcp.27782 [published Online First: 2018/12/07].
[14] M. Zhang, G. Hutter, S.A. Kahn, et al., Anti-CD47 treatment stimulates phagocytosis of glioblastoma by M1 and M2 polarized macrophages and promotes M1 polarized macrophages *in vivo*, PLoS One 11 (4) (2016), e0153550, https://doi.org/10.1371/journal.pone.0153550 [published Online First: 2016/04/20].
[15] C. Ecker, J.L. Riley, Translating *in vitro* T cell metabolic findings to *in vivo* tumor models of nutrient competition, Cell Metab. 28 (2) (2018) 190–195, https://doi.org/10.1016/j.cmet.2018.07.009 [published Online First: 2018/08/09].
[16] M.G.V. Heiden, R.J. DeBerardinis, Understanding the intersections between metabolism and cancer biology, Cell 168 (4) (2017) 657–669, https://doi.org/10.1016/j.cell.2016.12.039 [published Online First: 2017/02/12].
[17] M. Peng, D. Yang, Y. Hou, et al., Intracellular citrate accumulation by oxidized ATM-mediated metabolism reprogramming via PFKP and CS enhances hypoxic breast cancer cell invasion and metastasis, Cell Death Dis. 10 (3) (2019) 228, https://doi.org/10.1038/s41419-019-1475-7 [published Online First: 2019/03/10].
[18] A. Zambrano, M. Molt, E. Uribe, et al., Glut 1 in cancer cells and the inhibitory action of resveratrol as a potential therapeutic strategy, Int. J. Mol. Sci. 20 (13)

(2019), https://doi.org/10.3390/ijms20133374 [published Online First: 2019/07/22].
[19] A. Magi, M. Masselli, C. Sala, et al., The ion channels and transporters gene expression profile indicates a shift in excitability and metabolisms during malignant progression of Follicular Lymphoma, Sci. Rep. 9 (1) (2019) 8586, https://doi.org/10.1038/s41598-019-44661-x [published Online First: 2019/06/15].
[20] T. Yu, S. Gan, Q. Zhu, et al., Modulation of M2 macrophage polarization by the crosstalk between Stat6 and Trim24, Nat. Commun. 10 (1) (2019) 4353, https://doi.org/10.1038/s41467-019-12384-2 [published Online First: 2019/09/27].
[21] E.F. McKinney, J.C. Lee, D.R. Jayne, et al., T-cell exhaustion, co-stimulation and clinical outcome in autoimmunity and infection, Nature 523 (7562) (2015) 612–616, https://doi.org/10.1038/nature14468 [published Online First: 2015/07/01].
[22] M.G. Scherm, I. Serr, A.M. Zahm, et al., miRNA142-3p targets Tet2 and impairs Treg differentiation and stability in models of type 1 diabetes, Nat. Commun. 10 (1) (2019) 5697, https://doi.org/10.1038/s41467-019-13587-3 [published Online First: 2019/12/15].
[23] P. Li, X. Yang, Y. Cheng, et al., MicroRNA-218 increases the sensitivity of bladder cancer to cisplatin by targeting glut1, Cell Physiol. Biochem. 41 (3) (2017) 921–932, https://doi.org/10.1159/000460505 [published Online First: 2017/02/22].
[24] V. Prima, L.N. Kaliberova, S. Kaliberov, et al., COX2/mPGES1/PGE2 pathway regulates PD-L1 expression in tumor-associated macrophages and myeloid-derived suppressor cells, Proc. Natl. Acad. Sci. U. S. A. 114 (5) (2017) 1117–1122, https://doi.org/10.1073/pnas.1612920114 [published Online First: 2017/01/18].
[25] S.R. Gordon, R.L. Maute, B.W. Dulken, et al., PD-1 expression by tumour-associated macrophages inhibits phagocytosis and tumour immunity, Nature 545 (7655) (2017) 495–499, https://doi.org/10.1038/nature22396 [published Online First: 2017/05/18].
[26] A.I. Cioroianu, P.I. Stinga, L. Sticlaru, et al., Tumor microenvironment in diffuse large B-cell lymphoma: role and prognosis, Anal. Cell Pathol. 2019 (2019), 8586354, https://doi.org/10.1155/2019/8586354 (Amst)[published Online First: 2020/01/15].
[27] M.D. Buck, R.T. Sowell, S.M. Kaech, et al., Metabolic Instruction of Immunity, Cell 169 (4) (2017) 570–586, https://doi.org/10.1016/j.cell.2017.04.004 [published Online First: 2017/05/06].
[28] H. Jeong, S. Kim, B.J. Hong, et al., Tumor-associated macrophages enhance tumor hypoxia and aerobic glycolysis, Cancer Res. 79 (4) (2019) 795–806, https://doi.org/10.1158/0008-5472.CAN-18-2545 [published Online First: 2019/01/06].
[29] S. Qiu, L. Deng, X. Liao, et al., Tumor-associated macrophages promote bladder tumor growth through PI3K/AKT signal induced by collagen, Cancer Sci. 110 (7) (2019) 2110–2118, https://doi.org/10.1111/cas.14078 [published Online First: 2019/05/24].
[30] A. Hamidi, J. Song, N. Thakur, et al., TGF-beta promotes PI3K-AKT signaling and prostate cancer cell migration through the TRAF6-mediated ubiquitylation of p85alpha, Sci. Signal 10 (486) (2017), https://doi.org/10.1126/scisignal.aal4186 [published Online First: 2017/07/06].
[31] A. Pichard, S. Marcatili, J. Karam, et al., The therapeutic effectiveness of (177)Lu-lilotomab in B-cell non-Hodgkin lymphoma involves modulation of G2/M cell cycle arrest, Leukemia 34 (5) (2020) 1315–1328, https://doi.org/10.1038/s41375-019-0677-4 [published Online First: 2019/12/15].
[32] A. Roisman, G. Castellano, A. Navarro, et al., Differential expression of long non-coding RNAs are related to proliferation and histological diversity in follicular lymphomas, Br. J. Haematol. 184 (3) (2019) 373–383, https://doi.org/10.1111/bjh.15656 [published Online First: 2018/12/20].
[33] K. Nath, S.C. Law, M.B. Sabdia, et al., Intratumoral T cells have a differential impact on FDG-PET parameters in follicular lymphoma, Blood Adv. 5 (12) (2021) 2644–2649, https://doi.org/10.1182/bloodadvances.2020004051 [published Online First: 2021/06/23].
[34] L. Sun, H. Zhang, P. Gao, Metabolic reprogramming and epigenetic modifications on the path to cancer, Protein Cell 13 (12) (2022) 877–919, https://doi.org/10.1007/s13238-021-00846-7 [published Online First: 2021/05/30].
[35] H. Lemos, L. Huang, G.C. Prendergast, et al., Immune control by amino acid catabolism during tumorigenesis and therapy, Nat. Rev. Cancer 19 (3) (2019) 162–175, https://doi.org/10.1038/s41568-019-0106-z [published Online First: 2019/01/31].
[36] I. Vitale, G. Manic, L.M. Coussens, et al., Macrophages and metabolism in the tumor microenvironment, Cell Metab. 30 (1) (2019) 36–50, https://doi.org/10.1016/j.cmet.2019.06.001 [published Online First: 2019/07/04].
[37] Z. Yin, L. Bai, W. Li, et al., Targeting T cell metabolism in the tumor microenvironment: an anti-cancer therapeutic strategy, J. Exp. Clin. Cancer Res. 38 (1) (2019) 403, https://doi.org/10.1186/s13046-019-1409-3 [published Online First: 2019/09/15].
[38] M.F. Miniotis, V. Arunan, T.R. Eykyn, et al., MEK1/2 inhibition decreases lactate in BRAF-driven human cancer cells, Cancer Res. 73 (13) (2013) 4039–4049, https://doi.org/10.1158/0008-5472.CAN-12-1969 [published Online First: 2013/05/04].
[39] M. Broecker-Preuss, N. Becher-Boveleth, A. Bockisch, et al., Regulation of glucose uptake in lymphoma cell lines by c-MYC- and PI3K-dependent signaling pathways and impact of glycolytic pathways on cell viability, J. Transl. Med. 15 (1) (2017) 158, https://doi.org/10.1186/s12967-017-1258-9 [published Online First: 2017/07/21].
[40] S. Hu, R. Wang, M. Zhang, et al., BAFF promotes T cell activation through the BAFF-BAFF-R-PI3K-Akt signaling pathway, Biomed. Pharmacother. 114 (2019), 108796, https://doi.org/10.1016/j.biopha.2019.108796 [published Online First: 2019/03/29].
[41] M. Dreyling, A. Santoro, L. Mollica, et al., Long-term safety and efficacy of the PI3K inhibitor copanlisib in patients with relapsed or refractory indolent lymphoma: 2-year follow-up of the CHRONOS-1 study, Am. J. Hematol. 95 (4) (2020) 362–371, https://doi.org/10.1002/ajh.25711 [published Online First: 2019/12/24].
[42] J. Ding, Q. Gou, J. Jin, et al., Metformin inhibits PPARdelta agonist-mediated tumor growth by reducing Glut1 and SLC1A5 expressions of cancer cells, Eur. J. Pharmacol. 857 (2019), 172425, https://doi.org/10.1016/j.ejphar.2019.172425 [published Online First: 2019/06/01].